Non-linear dynamics of the fermion-boson model: interference between revivals and the transition to irregularity

1981 J. Phys. A: Math. Gen. 14 1383

(http://iopscience.iop.org/0305-4470/14/6/015)

J. Phys. A: Math. Gen. **14** (1981) 1383–1397. Printed in Great Britain

Non-linear dynamics of the fermion–boson model: interference between revivals and the transition to irregularity

H-I Yoo, J J Sanchez-Mondragon† and J H Eberly

Department of Physics and Astronomy, University of Rochester, Rochester, NY 14627, USA

Received 7 November 1980

Abstract. We extend recent studies of the quantised fermion–boson model. Parallel numeric and approximate analytic advances allow greater understanding of the 'collapse' regions between successive 'revivals' in the fermion energy evolution. We give an estimate of the time for the onset of continuous irregularity as a function of the average boson number.

1. Introduction

The Hamiltonian given in equation (1.1) is an extremely idealised model version of realistic Hamiltonians governing physical phenomena in various fields.

$$\hat{H} = \tfrac{1}{2}\hbar\omega_0\hat{\sigma}_3 + \hbar\lambda(\hat{\sigma}_+\hat{a} + \hat{a}^+\hat{\sigma}_-) + \hbar\omega\hat{a}^+\hat{a}. \tag{1.1}$$

For example, if the 'boson' operators $\hat{a}^+$ and $\hat{a}$ create and destroy photons and the 'fermion' operators $\hat{\sigma}_3$, $\hat{\sigma}_+$, $\hat{\sigma}_-$ represent a two-state atom or molecule, then $\hat{H}$ is known in quantum optics as the Jaynes–Cummings Hamiltonian (Jaynes and Cummings 1963, see also Jaynes 1958). There are analogues in spin–phonon resonance and quantum field theory (the static Lee model). Basically $\hat{H}$ can be said to describe any situation in which the absorption or emission of 'a' quanta causes the raising or lowering of the state of the 'σ' system.

Because of the mixture of 'boson' and 'fermion' degrees of freedom in $\hat{H}$, the associated dynamical problem is apparently essentially non-linear. Nevertheless, the model has commanded attention because it is both quantum mechanical and exactly solvable. That is, the exact eigenvalues and eigenstates of $\hat{H}$ have been long known (Jaynes 1958). Despite this, the dynamical behaviour of every operator in $\hat{H}$ has remained practically unknown (both qualitatively and quantitatively) until recently, except in specially restricted circumstances. Cummings (1965) first pointed out the importance of studies of the operator dynamics of the model under the assumption of an initially 'coherent' boson state, and it is in the case of a strongly excited initial coherent state that some progress has recently been made.

It has been shown (Eberly *et al* 1980) both numerically and approximately analytically that the fermion 'energy' or 'spin projection' signal, i.e. the expectation of the

† Mary Street Jenkins Foundation Fellow.

0305-4470/81/061383+15$01.50

operator $\hat{\sigma}_3(t)$, undergoes sinusoidal oscillation for a time of the order of λ^{-1}, and that these oscillations then 'collapse' to a value $\langle\hat{\sigma}_3(t)\rangle \simeq 0$. After a time long compared with λ^{-1} periodic 'revivals', packets of finite $\langle\hat{\sigma}_3(t)\rangle$ oscillation, subsequently occur. These spin signal revivals (which are not Poincaré recurrences) become less complete and begin to broaden, eventually overlapping each other at still longer times. These features are shown in figure 1.

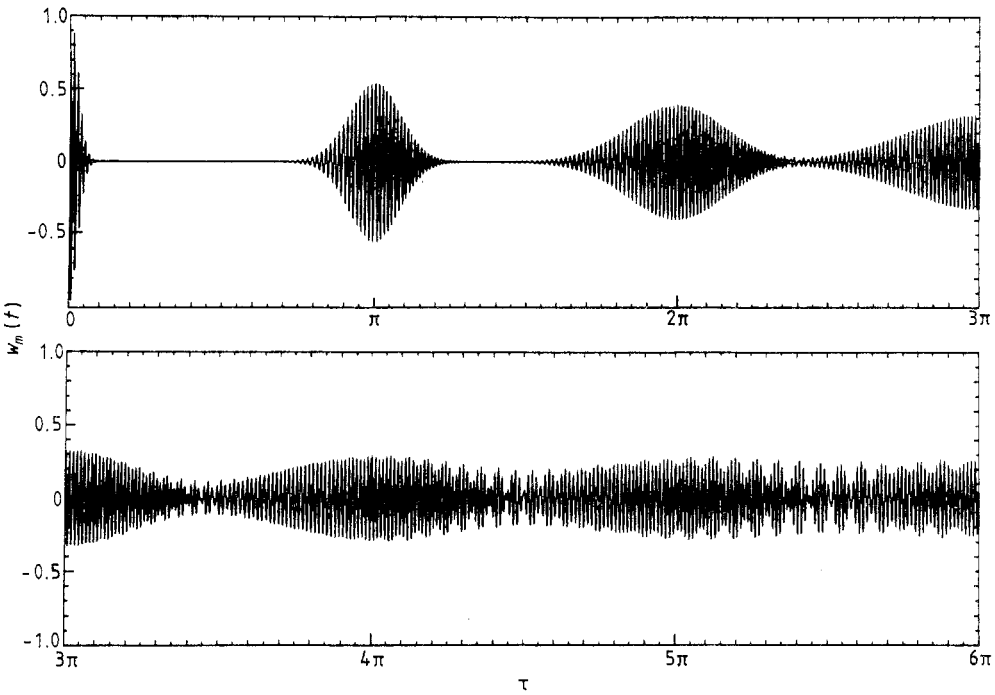

Figure 1. The inversion signal $w_m(t) = \langle\hat{\sigma}_3(t)\rangle/\langle\hat{\sigma}_3(0)\rangle$ as a function of the scaled time $\tau = \lambda t/2\sqrt{\bar{n}}$ when $\omega_0 = \omega$. $\langle\hat{\sigma}_3(0)\rangle$ is taken to be -1. Average boson number $\bar{n} = 40$. The time region shown in this figure is $0 \leqslant \tau \leqslant 6\pi$.

In the regions of revival overlap the envelope of the spin signal traces an irregular, quasi-chaotic curve. In this paper we undertake a re-examination of the time dependence of $\langle\hat{\sigma}_3(t)\rangle$ in this domain of irregularity. A systematic saddle point analysis of an approximate integral representation of $\langle\hat{\sigma}_3(t)\rangle$ is developed. It is found that there is a one-to-one correspondence between saddle points and signal revivals. This approach reveals that each revival packet of spin oscillations can be assigned its own oscillation frequency and leads to the prediction of beat phenomena in the regions of collapse between revivals. We estimate, as a function of average boson number, the time for the onset of beats and the time after which the beats degenerate into apparently continuous irregularity. These estimates are compared with the new numerical results valid for very long times.

Before proceeding to § 2, we briefly review the derivation of the expression for the spin signal. Our system consists of one two-level spin and a single mode of a boson field which interact with each other via the Hamiltonian given above in (1.1). In this Hamiltonian (Allen and Eberly 1975) $\hat{\sigma}_\pm \equiv \frac{1}{2}(\hat{\sigma}_1 \pm i\hat{\sigma}_2)$ and $\hat{\sigma}_j$ $(j = 1, 2, 3)$ are Pauli

matrices; and $\hat{a}$ and $\hat{a}^+$ are annihilation and creation operators of bosons with energy $\hbar\omega$. The detuning parameter Δ is defined as the difference between the spin and boson field mode frequencies

$$\Delta \equiv \omega_0 - \omega. \tag{1.2}$$

To indicate the initial spin state we use the letter m; e.g. $m = 1$ ($m = -1$) implies the spin is in the upper (lower) state. We assume the bosons are in a perfectly coherent state $|\alpha\rangle$ at $t = 0$. Then the Heisenberg equation of motion for the operator $\hat{\sigma}_3(t)$ leads to the following expression (Cummings 1965, Stenholm 1973, Meystre *et al* 1975, von Foerster 1975) for $W_m(t)$, the spin projection or spin 'inversion' (positive projection corresponding to an excited or 'inverted' spin)

$$\begin{aligned} W_m(t) &= \langle \alpha, m|\hat{\sigma}_3(t)|\alpha, m\rangle \\ &= \langle m|\hat{\sigma}_3(0)|m\rangle w_m(t) \end{aligned} \tag{1.3}$$

where $w_m(t)$ is the ratio of inversion to initial inversion

$$w_m(t) = \sum_{n=0}^{\infty} P(n, |\alpha|^2)[\Delta^2/\Omega_m^2(n) + (1 - \Delta^2/\Omega_m^2(n)) \cos(\Omega_m(n)t)]. \tag{1.4}$$

We shall call $w_m(t)$ the inversion signal from now on. Here the oscillation frequency $\Omega_m(n)$ is defined by

$$\Omega_m^2(n) = \Delta^2 + 4\lambda^2[n + \tfrac{1}{2}(m+1)] \tag{1.5}$$

and the weight function $P(n, |\alpha|^2)$ is Poissonian

$$P(n, |\alpha|^2) = \exp(-|\alpha|^2)|\alpha|^{2n}/n!. \tag{1.6}$$

2. Formulation of the saddle point approach

We are interested in the strong boson excitation case, so we evaluate equation (1.4) in the limit $|\alpha|^2 \equiv \bar{n} \gg 1$. First we separate $w_m(t)$ of equation (1.4) into two parts

$$w_m(t) = w_{m1} + w_{m2}(t) \tag{2.1}$$

where

$$w_{m1} = \sum_{n=0}^{\infty} P(n, \bar{n})\Delta^2/\Omega_m^2(n) \tag{2.2a}$$

and

$$w_{m2}(t) = \sum_{n=0}^{\infty} P(n, \bar{n})(1 - \Delta^2/\Omega_m^2(n)) \cos(\Omega_m(n)t). \tag{2.2b}$$

The evaluation of w_{m1} is straightforward, using the sharp peak of $P(n, \bar{n})$ at $n = \bar{n}$, and we obtain the result

$$w_{m1} \simeq \Delta^2/\Omega_m^2(\bar{n}). \tag{2.3}$$

The evaluation of $w_{m2}(t)$ can be obtained as follows. We introduce $y^2 = n/\bar{n}$ and rewrite (2.2*b*) as an integral:

$$w_{m2}(t) \simeq \left(\frac{2\bar{n}}{\pi}\right)^{1/2} \mathrm{Re} \int_0^{\infty} \exp(\bar{n} f(y; t))(1 - \Delta^2/\Omega_m^2(\bar{n}y^2))\, dy. \tag{2.4}$$

The weight factor $P(n, \bar{n}) = e^{-\bar{n}}\bar{n}^n/n!$ has a peak at $n = \bar{n}$ with a dispersion law $(\overline{n^2} - \bar{n}^2)^{1/2} = \sqrt{\bar{n}}$. Since $\bar{n} \gg 1$ and the main part of the summation is in the range between $\bar{n} - \sqrt{\bar{n}}$ and $\bar{n} + \sqrt{\bar{n}}$, we have used Stirling's formula for $n!$. The phase function is given by

$$f(y; t) = y^2(1 - 2 \ln y) - 1 + i\frac{\Omega_m(\bar{n}y^2)}{\bar{n}} t. \tag{2.5}$$

The saddle points y_0 of $f(y; t)$ are given by

$$\frac{\partial}{\partial y} f\Big|_{y=y_0} = 0$$

and this leads to the following equation

$$(y_0^2 + \delta_m^2)^{1/2} \ln y_0 = i\lambda t/2\sqrt{\bar{n}} \tag{2.6}$$

where

$$\delta_m^2 = [\Delta^2 + 2\lambda^2(m+1)]/4\lambda^2\bar{n}. \tag{2.7}$$

The saddle points y_0, which are solutions of equation (2.6), are infinite in number. However, it is shown in the appendix that for any given time t only those saddle points which have a norm close to unity ($|y_0| \sim 1$) give significant contributions and that the contributions from the remaining saddle points are negligible.

In the appendix we explain the details of our saddle point analysis. The result is that, in terms of the scaled time τ

$$\tau \equiv \lambda t/2\sqrt{\bar{n}} \tag{2.8}$$

and for the simplest case, $\Delta = 0$ and $m = -1$, we can express the inversion signal as a sum of contributions, one from each saddle point

$$w_m(t) = \sum_{y_0} \mathrm{Re} \frac{\exp(\bar{n}f(y_0; \tau) + i\alpha(y_0))}{[\varphi^2 + (1 + \ln \rho)^2]^{1/4}}. \tag{2.9}$$

Here f is given in (2.5), with $\Delta = 0$ and $m = -1$; $-2\alpha(y_0)$ is the angle of steepest descent at y_0

$$-2\alpha(y_0) \simeq \tan^{-1}(\tau) \tag{2.10}$$

and ρ and φ are the amplitude and phase of y_0

$$y_0 \equiv \rho\, e^{i\varphi}. \tag{2.11}$$

We find that the revivals occur at times $\tau = k\pi$, and that the kth saddle point† dominates the sum in equation (2.9) when $\tau \approx k\pi$. It is useful to define a local time ε_k

$$\varepsilon_k \equiv \tau - k\pi \tag{2.12}$$

associated with the kth saddle point when τ is in the neighbourhood of $k\pi$. Then the inversion signal (2.9) can be rewritten

$$w_m(t) = \sum_{k=0}^{\infty} U_m^{(k)}(\varepsilon_k) \tag{2.13}$$

where

$$U_m^{(k)} = [(1 + \ln \rho)^2 + \varphi^2]^{-1/4} \exp(-\Psi(y_0; \tau)) \cos \Phi(y_0; \tau). \tag{2.14}$$

† See the explanation below (A.2*b*) in the appendix, for the labelling of the saddle points.

Here, y_0 on the right-hand side of (2.14) is the kth saddle point at time τ, and ε_k is the corresponding local time. We shall call $U_m^{(k)}$ the kth revival signal.

Finally, we can give explicit expressions for the individual revival signals in terms of k and ε_k:

$$U_m^{(k)}(\varepsilon_k) \simeq (1+\tau^2)^{-1/4} \exp(-\Psi_k(\varepsilon_k)) \cos \Phi_k(\varepsilon_k) \tag{2.15}$$

$$\Psi_k(\varepsilon_k) = \frac{2\bar{n}}{1+(k\pi)^2}\,\varepsilon_k^2 + O(\varepsilon_k^3) \tag{2.16}$$

$$\Phi_k(\varepsilon_k) = \bar{n}\left(2k\pi + 4\varepsilon_k + \frac{2k\pi}{1+(k\pi)^2}\,\varepsilon_k^2\right) + \alpha_k + O(\varepsilon_k^3) \tag{2.17}$$

$$\alpha_k \simeq -\tfrac{1}{2}\tan^{-1}(\tau). \tag{2.18}$$

Here we have eliminated a factor $(-1)^k$ from $\Phi_k(\varepsilon_k)$ since cos is an even function.

Note that we are working with the scaled time τ defined by equation (2.9) and in the original time scale the kth revival time t_{0k} and its local time s_k are given by

$$t_{0k} = \frac{2\sqrt{\bar{n}}}{\lambda}\,k\pi \qquad s_k = \frac{2\sqrt{\bar{n}}}{\lambda}\,\varepsilon_k. \tag{2.19}$$

As a function of time τ, the envelope of $U_m^{(k)}(\varepsilon_k)$ is Gaussian in form, centred at $\tau = k\pi$ with its width

$$\Delta\tau_k = 2\left(\frac{1+(k\pi)^2}{2\bar{n}}\right)^{1/2} \tag{2.20a}$$

and its maximum height

$$h_k = [1+(k\pi)^2]^{-1/4}. \tag{2.20b}$$

Figure 2 shows the envelopes of $U^{(k)}$ that contribute to $w_m(t)$. The $U_m^{(k)}$ are well separated from each other for k which satisfy the inequality $k < \sqrt{\bar{n}}/2$. In other words, each revival signal is well isolated from the others in the time region where $\tau < \frac{1}{2}\pi\sqrt{\bar{n}}$.

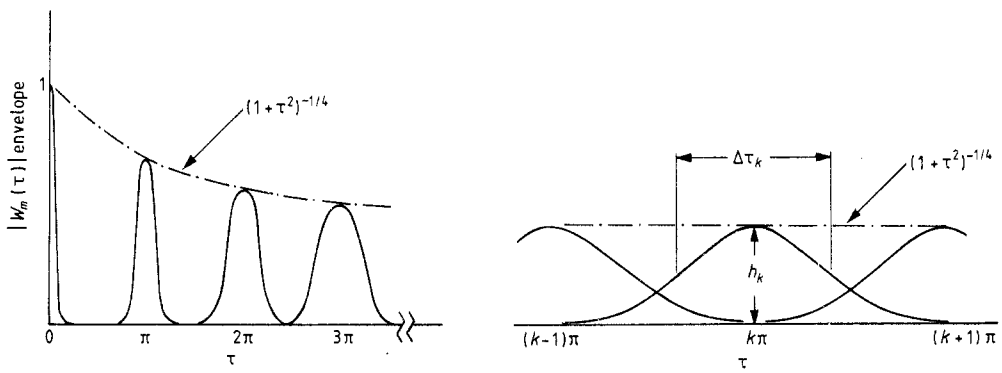

Figure 2. The superposition of the envelopes of several $U_m^{(k)}$. The peak around $\tau = k\pi$ ($k = 0, 1 \ldots$) corresponds to the kth revival signals $U_m^{(k)}$. For τ smaller than the critical value τ_{c_1} defined in equation (2.21) each revival signal is well separated from its neighbours.

It is useful, for later considerations, to introduce two critical times τ_{c_1} and τ_{c_2} defined by

$$\tau_{c_1} \equiv \tfrac{1}{2}\pi\sqrt{\bar{n}} \tag{2.21}$$

$$\tau_{c_2} \equiv 4\tau_{c_1} = 2\pi\sqrt{\bar{n}}. \tag{2.22}$$

When τ exceeds τ_{c_1}, a neighbouring pair of revival signals starts overlapping in their tails. This overlapping becomes more prominent as τ gets larger and after $\tau = \tau_{c_2}$ not only that pair but also second nearest or further neighbours participate in the inversion signal. We shall show in § 3 that an interference between adjacent revival signals does occur in the region of overlap.

Finally, we lift the restriction to $\Delta = 0$, and give the results for small Δ corresponding to those given above. First we go back to equation (2.6)

$$y_0 \ln y_0 = i\tau(1 + \delta_m^2 y_0^{-2})^{-1/2}.$$

If $\tau(1+\delta_m^2)^{-1/2} = k\pi$, then $y_0 = \exp[i(-1)^k k\pi]$ is a solution of equation (2.6). In the case $\Delta = 0$, we know that $y_0 = \rho\, e^{i\varphi}$ does not change much in the range $|\varepsilon_k| \leqslant \pi$ for $k\pi \gg 1$. We may expect the characteristic features not to change significantly from the case $\delta_m = 0$ to the case $\delta_m^2 \ll 1$ so we replace y_0^{-2} in the root of equation (2.6) by unity

$$y_0 \ln y_0 = i\tau(1 + \delta_m^2)^{-1/2}. \tag{2.23}$$

Comparing equation (2.23) with equation (A.1) we see immediately that the effect of small detunings is expressible in terms of a 'rescaling' of time

$$\tau \to \tilde{\tau} \equiv \tau(1+\delta_m^2)^{-1/2}.$$

Hence it is a straightforward matter to extend the procedure of the previous section to the small δ_m case. One obtains the results:

$$w_m(t) = \delta^2(1+\delta^2)^{-1} + \sum_{k=0}^{\infty} U_m^{(k)}(\tilde{\varepsilon}_k) \tag{2.24}$$

$$U_m^{(k)}(\tilde{\varepsilon}_k) = (1+\delta^2)^{-1}[1+(1+\delta_m^2)^{-3}\tau^2]^{-1/4} \exp(-\Psi_k(\tilde{\varepsilon}_k)) \cos \Phi_k(\tilde{\varepsilon}_k) \tag{2.25}$$

$$\Psi_k(\tilde{\varepsilon}_k) = \frac{2\bar{n}}{1+(k\pi)^2}\,\tilde{\varepsilon}_k^2 \tag{2.26}$$

$$\Phi_k(\tilde{\varepsilon}_k) = \bar{n}\left((2+4\delta_m^2)k\pi + 4\tilde{\varepsilon}_k + \frac{2k\pi}{1+(k\pi)^2}\,\tilde{\varepsilon}_k^2\right) + \alpha_k \tag{2.27}$$

$$\alpha_k \simeq -\frac{1}{2}\tan^{-1}\left(\frac{\tau}{(1+\delta_m^2)^{3/2}}\right) \tag{2.28}$$

where δ_m and δ are defined by

$$\delta_m^2 \equiv [\Delta^2 + 4\lambda^2 \tfrac{1}{2}(m+1)]/4\lambda^2\bar{n}$$

and

$$\delta^2 \equiv \Delta^2/4\lambda^2 N_{\bar{n}m}. \tag{2.29}$$

Here $N_{\bar{n}m}$ is the 'excitation number' of the initial averaged boson number $\bar{n}$ for the coupled system

$$N_{\bar{n}m} = \bar{n} + \tfrac{1}{2}(m+1) \tag{2.30}$$

and $\tilde{\varepsilon}_k$ in the above is the 'rescaled' local time defined by

$$\tilde{\tau} \equiv \tau(1+\delta_m^2)^{-1/2} = k\pi + \tilde{\varepsilon}_k. \tag{2.31}$$

Correspondingly, actual time t can be separated into two parts $t = t_{0,k} + s_k$, $t_{0,k}$ being the time when the kth saddle point passes the $\rho = 1$ line and s_k being kth local time measured from $t_{0,k}$. Then the kth revival time $t_{0,k}$ is given by

$$t_{0,k} = (1+\delta^2)^{1/2}\, 2\lambda^{-1}\sqrt{N_{\bar{n}m}}\, k\pi \tag{2.32}$$

and s_k is given in terms of $\tilde{\varepsilon}_k$ by

$$s_k = (1+\delta^2)^{1/2}\, 2\lambda^{-1}\sqrt{N_{\bar{n}m}}\, \tilde{\varepsilon}_k. \tag{2.33}$$

In equation (2.27) the common factor $(-1)^k$ has again been eliminated from Φ_k.

The effect of small detuning can be seen to have three aspects:

(i) non-zero time average of $w_m(t)$,

(ii) decrease of height of envelope of revival signal and

(iii) delay of revival time by the factor $(1+\delta^2)^{1/2}$.

The initial spin state also affects the revival time, and the width and phase of the revival signals through $N_{\bar{n}m}$.

3. Interference between revival signals

As mentioned below equation (2.22), § 2, two adjacent revival signals overlap each other when τ is in the region $\tau_{c_1} < \tau < \tau_{c_2}$. The phase of each revival signal has a distinctive time dependence, as seen in equation (2.27). Therefore, we may expect to see an interference phenomenon in the overlapped region. For simplicity we consider the case of $\Delta = 0$ and $m = -1$. The frequency of the kth revival signal at local time ε_k, $\omega_k(\varepsilon_k)$, can be calculated from equation (2.17)

$$\omega_k(\varepsilon_k) = \frac{\mathrm{d}}{\mathrm{d}\varepsilon_k}\Phi_k(\varepsilon_k) = 4\bar{n} + \frac{4\bar{n}k\pi}{1+(k\pi)^2}\,\varepsilon_k + \frac{\mathrm{d}\alpha_k}{\mathrm{d}\varepsilon_k} + \mathrm{O}(\varepsilon_k^2). \tag{3.1}$$

Equation (3.1) shows that ω_k depends on both k and ε_k. Under the condition $\bar{n} \gg 1$ the third term, $\mathrm{d}\alpha_k/\mathrm{d}\varepsilon_k$, can be neglected to simplify our discussion.

At the region around $\tau = (k+\frac{1}{2})\pi$ where $\tau_{c_1} < \tau < \tau_{c_2}$ there coexist the kth and the $(k+1)$th revival signals with roughly the same amplitudes. Therefore, in this region the formation of beats will be expected in the inversion due to the frequency difference of these two revival signals. Let

$$\tau = (k+\tfrac{1}{2})\pi + \beta; \tag{3.2}$$

then the kth and the $(k+1)$th local times, ε_k and ε_{k+1} respectively, are given by

$$\varepsilon_k = \tfrac{1}{2}\pi + \beta \qquad \text{and} \qquad \varepsilon_{k+1} = -\tfrac{1}{2}\pi + \beta. \tag{3.3}$$

The beat frequency $\omega_{\mathrm{beat}}(\beta)$ and the frequency of basic oscillation $\omega_{\mathrm{osc}}(\beta)$ are given by

$$\omega_{\mathrm{beat}}(\beta) = \tfrac{1}{2}|\omega_k(\tfrac{1}{2}\pi+\beta) - \omega_{k-1}(-\tfrac{1}{2}\pi+\beta)| \tag{3.4}$$

$$\omega_{\mathrm{osc}}(\beta) = \tfrac{1}{2}(\omega_k(\tfrac{1}{2}\pi+\beta) + \omega_{k+1}(-\tfrac{1}{2}\pi+\beta)). \tag{3.5}$$

When $(k\pi)^2 \gg 1$, $\omega_{\text{beat}}(\beta)$ and $\omega_{\text{osc}}(\beta)$ are given by

$$\omega_{\text{beat}}(\beta) \simeq \bar{n}\frac{2k+1+2\beta/\pi}{k(k+1)} \tag{3.6}$$

$$\omega_{\text{osc}}(\beta) \simeq \bar{n}\left(4+\frac{1+(2k+1)2\beta/\pi}{k(k+1)}\right). \tag{3.7}$$

When $\beta \ll \frac{1}{2}\pi$, the ratio of ω_{osc} to ω_{beat} is given by

$$\frac{\omega_{\text{osc}}}{\omega_{\text{beat}}} \simeq \frac{4k(k+1)}{2k+1}. \tag{3.8}$$

Equation (3.8) gives quite good quantitative agreement with new results obtained from computer summation of equation (1.4). As an example, in figure 3 we show the beats in the inversion between the kth and the $(k+1)$th revivals for $\sqrt{\bar{n}} = 7.5$, found by numerical summation. The number of oscillations within each beat envelope, near the centre of the beat regions, agrees very well with the ratio predicted by equation (3.8).

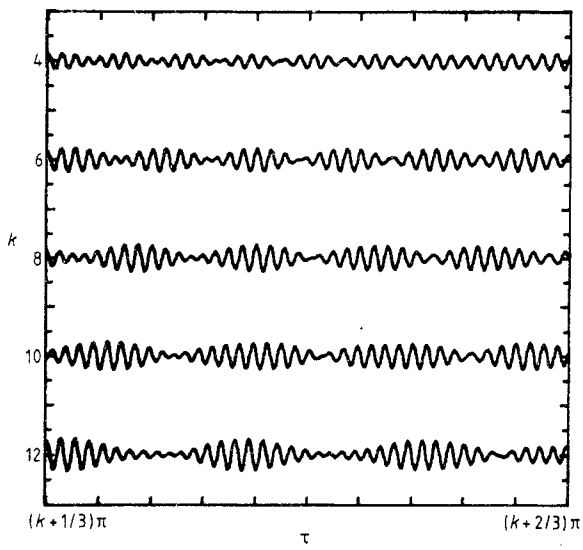

Figure 3. The inversion signal obtained from computer summation of equation (1.4). The time regions shown in the figure are the regions between successive revivals, beginning with the fourth, which is the case for which the two adjacent revival signals just start to overlap in their tails, for the given value $(\bar{n})^{1/2} = 7.5$. ($\Delta = 0$ and $m = -1$.)

Furthermore, in figure 4 we show the inversion computed from the exact sum (1.4) and computed from the superposition (2.13) and the difference between these two in the time regions (*a*) $6\pi \leqslant \tau \leqslant 7\pi$ and (*b*) $18\pi \leqslant \tau \leqslant 19\pi$ for $\bar{n} = 40$ under the conditions $\Delta = 0$ and $m = -1$. The inversion signal in the range (*a*) is made essentially by two revivals $U^{(6)}$ and $U^{(7)}$. On the other hand, the one in the range (*b*) consists of six or seven $U^{(k)}$. As is clearly seen in figure 4, the agreement between the two expressions (1.4) and (2.13) of the inversion for $\delta_m = 0$ is remarkably good, and this agreement seems to continue at even longer time. (We have checked up to four hundred revival times, i.e. $\tau = 400\pi$, and found no sign of deviation from this tendency.) Moreover, it

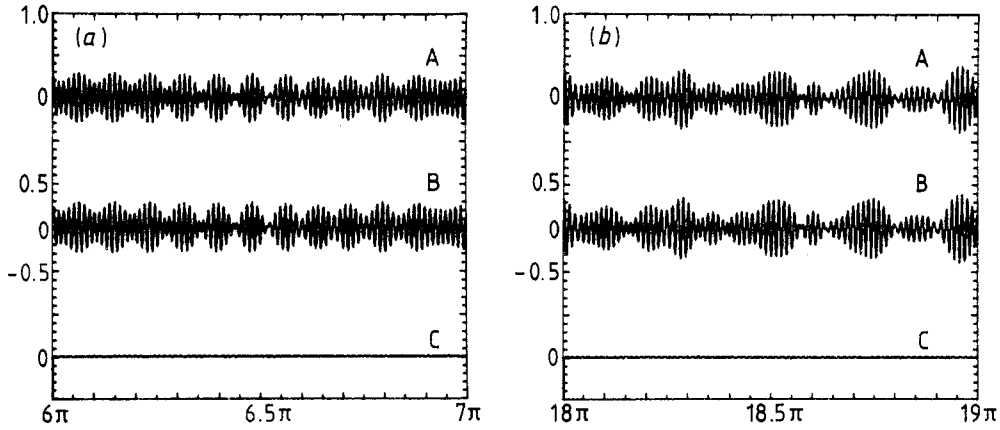

Figure 4. The inversion signal obtained from computer summation for $\delta_m = 0$ (i.e. $\Delta = 0$ and $m = -1$). The time interval is appropriate to show the transition from beating between revivals to apparently continuous irregularity. The average boson number is $\bar{n} = 40$. The time regions are (*a*) $6\pi \leqslant \tau \leqslant 7\pi$ and (*b*) $18\pi \leqslant \tau \leqslant 19\pi$. The graphs indicate the inversion signal computed from: A the exact sum (1.4) and B the superposition of revival signals (2.27). Graph C is the difference between these two.

has been confirmed by numerical comparison that the difference between (1.4) and (2.13) becomes smaller as $\bar{n}$ increases, as is expected. A brief comparison of figures 4 and 5 will give a reasonably good impression of this effect.

4. Conclusion and discussion

We have shown that $w_m(t)$, the ratio of inversion to initial inversion, is expressed as a superposition of revival signals, $U_m^{(k)}(\varepsilon_k)$ when $\bar{n} \gg 1$. As a function of time, the envelope of $U_m^{(k)}$ takes its maximum value h_k when $\tau = k\pi$. The time separation

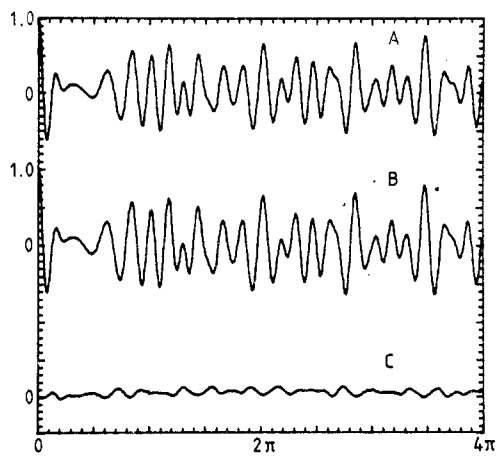

Figure 5. The inversion signal for $\bar{n} = 3$ for $\delta_m = 0$. The time range is $0 \leqslant \tau \leqslant 4\pi$. The graphs labelled A, B and C have the same meaning as those in figure 4.

between succeeding revivals $U_m^{(k+1)}$ and $U_m^{(k)}$, namely $(k+1)\pi - k\pi = \pi$, does not depend on k. In this sense the inversion signal is periodic. This is intimately related with the discreteness of the constituent oscillators in w_m, i.e. the left-hand side of equation (1.4). This periodicity of revivals, however, will be concealed after a certain time, after $\tau \approx \tau_{c_1}$, because of the overlapping of adjacent revivals.

The width of the kth revival signal $U_m^{(k)}$ is proportional to $k\pi$ when $(k\pi)^2 \gg 1$ (equation (2.20a)). This fact may be related to the motion of the kth saddle point along its branch: when $\tau = k\pi$ this saddle point is on the $\rho = 1$ line. Using equations (A.17) and (A.6) we can calculate the 'speed' v_k of the saddle point when it crosses the $\rho = 1$ line

$$v_k \simeq \left.\frac{\mathrm{d}\rho}{\mathrm{d}\tau}\right|_{\tau = k\pi} = \rho_1 \simeq \frac{1}{k\pi}. \tag{4.1}$$

The 'speed' v_k is inversely proportional to $k\pi$. On the other hand, the exponent in equation (A.12) is approximately a function of ρ only, since φ does not change so much compared with the change of ρ when $\rho \simeq 1$. Since this exponent has its minimum at $\rho = 1$ and grows larger when $|\rho - 1|$ increases, as mentioned below equation (A.16), a revival signal is appreciable only when the corresponding saddle point is in the range

$$1 - \Delta\rho \lesssim \rho \lesssim 1 + \Delta\rho. \tag{4.2}$$

Here $\Delta\rho$ can be evaluated by the condition

$$\Psi \simeq \bar{n}\{1 + (1 \pm \Delta\rho)^2[2\ln(1 \pm \Delta\rho) - 1]\} = 1 \tag{4.3}$$

and this gives

$$\Delta\rho = \frac{1}{2\sqrt{\bar{n}}}. \tag{4.4}$$

The time interval during which the kth saddle point stays in the region (4.2) is given by

$$\Delta\tau_k' \simeq (2\Delta\rho)/v_k \simeq k\pi/\sqrt{\bar{n}}. \tag{4.5}$$

This $\Delta\tau_k'$ coincides with the width $\Delta\tau_k$ of the kth revival signal given by equation (2.20a) except for a factor $\sqrt{2}$.

The number of saddle points found in the range (4.2) at a given time τ increases as τ becomes large, and these saddle points contribute to the inversion signal simultaneously with their distinctive phases. In the time range $\tau_{c_1} \lesssim \tau \lesssim \tau_{c_2}$, two (or at most three) saddle points stay in the range (4.2) for a given time and clear beats will be observed in the region just between two adjacent revival signals. This regular beat phenomenon, however, will become obscure after a time $\tau \simeq \tau_{c_2}$, and regularity will be replaced by apparent irregularity of the envelope of the inversion signal as time goes on, as is shown in figure 4. This irregularity is nothing but a result of a superposition of many revival signals, each of which has a distinctive time-dependent frequency.

An analytical expression for $w_m(t)$ is also given in the paper of Narozhny *et al* (1980). Their method is basically the same as ours, but their treatment is essentially a first-order 'perturbation' in the parameter ε_k. Then $w_m(t)$ is written as a single function just like one of the $U^{(k)}$ here, but with phase and exponent periodic in time. This periodicity was an *ad hoc* addition to the theory, designed to allow the contribution from a single saddle point to govern $w_m(t)$ at all times. On the other hand, in this paper we treat all the saddle points equally. As a result $w_m(t)$ is written as a superposition of

all $U^{(k)}$, where the perturbation is carried out up to the second order of ε_k. It turns out that the second-order term of ε_k in the phase Φ_k is essential to explain the interference effect between revival signals, an effect missed in the earlier analysis. We see now that the validity of the expression for $w_m(t)$ in Narozhny *et al* (1980) is restricted to the time region $0 \leqslant \tau \leqslant \tau_{c_1}$.

When τ is sufficiently larger than τ_{c_2}, we can consider a frequency distribution associated with the superposed $U^{(k)}$ at time τ,

$$g(\omega;\tau) \propto \sum_k (\text{magnitude of } U^{(k)} \text{ at } \tau) \times \delta(\omega - \omega_k(\varepsilon_k)) \tag{4.6}$$

where $\omega_k(\varepsilon_k)$ is given by (3.1). This $g(\omega;\tau)$ may represent characteristic features of the regularity–irregularity problem of the inversion signal. $g(\omega;\tau)$ is centred at $\omega \simeq 4\bar{n}$ with its width $\Delta\omega \simeq 4\sqrt{2\bar{n}}$. The centre and the width are nearly constant in time, though the $\omega_k(\varepsilon_k)$ themselves are time dependent. The number of ω_k which are significant in $g(\omega;\tau)$ is finite but increases as τ increases. In this sense we may say the 'degree' of irregularity of the inversion signal grows as time goes by.

Finally, we should mention that the step (2.2*b*) → (2.4), i.e. the replacement of the original summation by an integral, is not valid when t is not small, because of the phase part $\exp(i\Omega_m(n)t)$. Nevertheless, based on the extremely good agreement between the original summation form (1.4) and our result (2.13), we may claim that the saddle point method brings back the phase information which was lost by the step from (2.2*b*) to (2.4).

Acknowledgments

The research reported here was partially supported by the US Department of Energy under Contract No DE-AC03-76DP01118.

Appendix

We consider the simplest case where $\Delta = 0$ and $m = -1$. In this case $\delta_m = 0$ and equation (2.6) becomes

$$y_0 \ln y_0 = i\tau \tag{A.1}$$

where τ is a scaled time defined by

$$\tau \equiv \lambda t / 2\sqrt{\bar{n}}. \tag{2.8}$$

The solutions y_0 of equation (A.1) are complex in general, and if we write

$$y_0 = \rho\, e^{i\varphi} \tag{2.11}$$

then equation (A.1) reduces to two coupled equations

$$\rho \ln \rho = \tau \sin \varphi \tag{A.2a}$$

$$\rho = \tau \cos \varphi / \varphi. \tag{A.2b}$$

Figure 6 shows the graphs of the two functions $\rho = \exp(\varphi \tan \varphi)$ and $\rho = \tau \cos \varphi / \varphi$, which are equivalent to the set of equations (A.2*a*) and (A.2*b*), for $\tau = 1, 2\pi$ and 3π. The graph of the function $\rho = \exp(\varphi \tan \varphi)$ consists of an infinite number of branches

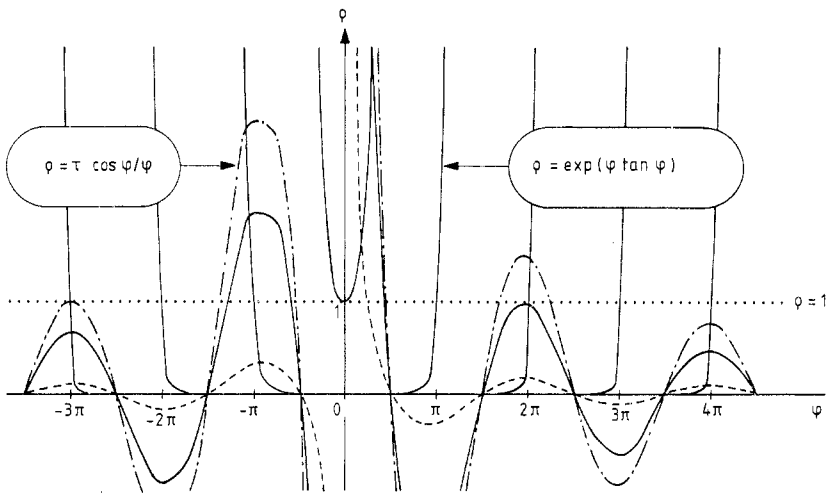

Figure 6. Figure 6. Solution curves for $\rho = \exp(\varphi \tan \varphi)$ and $\rho = \tau(\cos \varphi/\varphi)$ for three different values of τ: $\tau = 1, 2\pi$ and 3π. The intersections of the solution curves give the locations of the saddle points y_0 for these values of τ.

which are disconnected from each other. We shall call the kth branch the one which passes the point $(\rho = 1, \varphi = (-1)^k k\pi)$ where k is a non-negative integer. All the saddle points are on these branches. We shall also call the kth saddle point the one which is on the kth branch. As seen in figure 6, each saddle point moves upward (in the direction of increasing ρ) along its branch as time goes on, starting from $\rho = 0$, except for the zeroth saddle point which starts at $\rho = 1$ at time $\tau = 0$.

Now we separate time t into two parts

$$t = t_0 + s \tag{A.3}$$

where t_0 is some fixed time and s is the time measured from t_0. Correspondingly we write τ as a sum of two parts

$$\tau = \tau_0 + \varepsilon \tag{A.4}$$

where τ_0 and ε are given by

$$\tau_0 = \frac{\lambda t_0}{2\sqrt{\bar{n}}} \qquad \text{and} \qquad \varepsilon = \frac{\lambda s}{2\sqrt{\bar{n}}}. \tag{A.5}$$

We call ε (or s) local time. We use ε as an expansion parameter and write expansions for ρ and φ as

$$\rho = \rho(\tau_0 + \varepsilon) = \rho_0(\tau_0) + \varepsilon\rho_1(\tau_0) + \varepsilon^2\rho_2(\tau_0) + \ldots \tag{A.6}$$

$$\varphi = \varphi(\tau_0 + \varepsilon) = \varphi_0(\tau_0) + \varepsilon\varphi_1(\tau_0) + \varepsilon^2\varphi_2(\tau_0) + \ldots . \tag{A.7}$$

Substitution of equations (A.4), (A.6) and (A.7) into equations (A.2a) and (A.2b) gives the following expressions for the first several coefficients

$$\rho_0 = \tau_0 \cos \varphi_0/\varphi_0 \qquad \rho_0 \ln \rho_0 = \tau_0 \sin \varphi_0 \tag{A.8a}$$

$$\varphi_1 = \frac{\varphi_0}{\tau_0[\varphi_0^2 + (1+\ln\rho_0)^2]}$$
$$\rho_1 = \rho_0[\varphi_0^2 + (1+\ln\rho_0)\ln\rho_0]\varphi_1/\varphi_0 \tag{A.8b}$$

$$\varphi_2 = -(\varphi_0/A)[\varphi_0^4 + \varphi_0^2(2\ln^2\rho_0 + 6\ln\rho_0 + 5) + \ln\rho_0(4+\ln\rho_0)(1+\ln\rho_0)^2] \tag{A.8c}$$

$$\rho_2 = -\frac{\rho_0}{A(1+\ln\rho_0)}[\varphi_0^4(1+\ln\rho_0)(2+\ln\rho_0) + \varphi_0^2(-1+2\ln\rho_0)(2+\ln\rho_0) + \ln^2\rho_0(1+\ln\rho_0)^4]$$

where

$$A \equiv 2\tau_0^2[\varphi_0^2 + (1+\ln\rho_0)^2]^3.$$

Given τ_0, equations (A.8*a*), (A.8*b*) and (A.8*c*) determine the zeroth, the first-order and the second-order solutions of all the saddle points respectively.

For the case of $\Delta = 0$ and $m = -1$ equations (2.4) and (2.5) become

$$w_m(t) = w_{m2}(t) = \sum_{y_0} \mathrm{Re}\,\frac{\exp(\bar{n}f(y_0;\tau) + \mathrm{i}\alpha(y_0))}{[\varphi^2 + (1+\ln\rho)^2]^{1/4}} \tag{A.9}$$

where

$$f(y_0;\tau) = y_0^2(1 - 2\ln y_0) - 1 + \mathrm{i}4y_0\tau \tag{A.10}$$

and $-2\alpha(y_0)$ is the angle of steepest descent at the point y_0 and is given by

$$-2\alpha(y_0) \simeq \tan^{-1}(\tau). \tag{2.10}$$

The summation in equation (A.9) goes over all the saddle points y_0 at time τ, and it indicates that $w_m(t)$ is a superposition of the contributions of the individual saddle points.

We separate the exponent in equation (A.9) into real and imaginary parts

$$\bar{n}f(y_0;\tau) + \mathrm{i}\alpha(y_0) = -\Psi(y_0;\tau) + \mathrm{i}\Phi(y_0;\tau) \tag{A.11}$$

where

$$\Psi(y_0;\tau) = \bar{n}(1 + 2\rho^2\ln\rho - \rho^2\cos 2\varphi) \tag{A.12}$$

and

$$\Phi(y_0;\tau) = \bar{n}\rho^2(2\varphi + \sin 2\varphi) + \alpha(y_0). \tag{A.13}$$

Here we have used equations (A.2) to simplify the expressions of Ψ and Φ. The imaginary part Φ gives the phase of the revival signal of the atomic inversion, and equation (A.9) becomes

$$w_m(t) = \sum_{y_0} [\varphi^2 + (1+\ln\rho)^2]^{-1/4} \exp(-\Psi(y_0;\tau)) \cos\Phi(y_0;\tau). \tag{2.9}$$

If we make a Taylor expansion of Ψ and Φ in terms of ε, we reach the following expressions by using equations (A.6) and (A.7):

Exponent

$$\begin{aligned}
&\Psi(y_0;\tau) = \bar{n}(\psi_0(\tau_0) + \varepsilon\psi_1(\tau_0) + \varepsilon^2\psi_2(\tau_0) + \ldots) \\
&\psi_0 = 1 + 2\rho_0^2 \ln\rho_0 - \rho_0^2 \cos 2\varphi_0 \\
&\psi_1 = 2\rho_0\rho_1 + 4\rho_0\rho_1 \ln\rho_0 - 2\rho_0\rho_1 \cos 2\varphi_0 + 2\rho_0^2\varphi_1 \sin 2\varphi_0 \\
\psi_2 = {} & \rho_1^2(3 + 2\ln\rho_0) + 2\rho_0\rho_2(1 + 2\ln\rho_0) - (\rho_1^2 + 2\rho_0\rho_2 - 2\rho_0^2\varphi_1^2)\cos 2\varphi_0 \\
&+ (4\rho_0\rho_1\varphi_1 + 2\rho_0^2\varphi_2)\sin 2\varphi_0
\end{aligned} \tag{A.14}$$

Phase

$$\begin{aligned}
&\Phi(y_0;\tau) = \bar{n}(Y_0(\tau_0) + \varepsilon Y_1(\tau_0) + \varepsilon^2 Y_2(\tau_0) + \ldots) + \alpha(y_0) \\
&Y_0 = 2\varphi_0 + \sin 2\varphi_0 \\
&Y_1 = 2\rho_0\rho_1(2\varphi_0 + \sin 2\varphi_0) + 2\rho_0^2\varphi_1(1 + \cos 2\varphi_0) \\
Y_2 = {} & (\rho_1^2 + 2\rho_0\rho_2)(2\varphi_0 + \sin 2\varphi_0) + 4\rho_0\rho_1\varphi_1(1 + \cos 2\varphi_0) \\
&+ 2\rho_0^2[\varphi_2(1 + \cos 2\varphi_0) - \varphi_1^2 \sin 2\varphi_0].
\end{aligned} \tag{A.15}$$

Since any saddle point y_0 can be labelled by a non-negative integer k, we can write equation (2.9) as

$$w_m(t) = \sum_{k=0}^{\infty} U_m^{(k)}(\varepsilon_k) \tag{2.13}$$

and

$$U_m^{(k)}(\varepsilon_k) = [\varphi^2 + (1 + \ln\rho)^2]^{-1/4} \exp(-\Psi(y_0;\tau)) \cos\Phi(y_0;\tau). \tag{A.16}$$

Here y_0 in the right-hand side of equation (A.16) is the kth saddle point at time τ and ε_k is the local time for this branch. We name $U_m^{(k)}$ the kth revival signal. On the other hand, it can be shown that for $\tau \geq 0$ the exponent $\Psi(y_0;\tau)$ given by equation (A.12), when it is considered as a function of ρ, decreases monotonically for $\rho < 1$, increases monotonically for $\rho > 1$ and takes its minimum value zero at $\rho = 1$: $\Psi(y_0;\tau)|_{\min} = 0$. Since $\rho = 1$ corresponds to $\tau = k\pi$ if y_0 in $\Psi(y_0;\tau)$ is the kth saddle point, this analysis suggests that the proper choice of τ_0 is $k\pi$ for the kth saddle point. Then the local time for this saddle point, ε_k, is given by

$$\varepsilon_k = \tau - k\pi \tag{2.12}$$

i.e. ε_k is the (kth) local time measured from the instant when the kth saddle point passes the $\rho = 1$ line (in figure 6). With the choice $\tau_0 = k\pi$ for the kth saddle point equation (A.8) gives

$$\begin{aligned}
&\rho_0 = 1 \qquad \varphi_0 = (-1)^k k\pi \qquad \text{zeroth order} \\
&\rho_1 = \frac{k\pi}{1 + (k\pi)^2} \qquad \varphi_1 = \frac{(-1)^k}{1 + (k\pi)^2} \qquad \text{first order} \\
&\rho_2 = \frac{1 - (k\pi)^2}{[1 + (k\pi)^2]^3} \qquad \varphi_2 = (-1)^{k+1}\frac{k\pi[5 + (k\pi)^2]}{2[1 + (k\pi)^2]^3} \qquad \text{second order.}
\end{aligned} \tag{A.17}$$

The radius of convergence of expansions (A.6) and (A.7) depends on τ_0 and for $k \geq 2$, $|\varepsilon_k|$ may well be taken up to π. The larger the value of k, the larger the radius of convergence.

Substitution of equation (A.17) into equations (A.14) and (A.15) gives expressions for the exponent Ψ and phase Φ which belong to $U_m^{(k)}$ in terms of ε_k and k. Those are given by equations (2.16) and (2.17).

References

Allen L and Eberly J H 1975 *Optical Resonance and Two-Level Atoms* (New York: Wiley) § 7
Cummings F W 1965 *Phys. Rev.* **140** A1051–6
Eberly J H, Narozhny N B and Sanchez-Mondragon J J 1980 *Phys. Rev. Lett.* **44** 1323–6
von Foerster T 1975 *J. Phys. A: Math. Gen.* **8** 95–102
Jaynes E T 1958 *Microwave Laboratory Report* Stanford University
Jaynes E T and Cummings F W 1963 *Proc. IEEE* **51** 89–109
Meystre P, Geneux E, Quattropani A and Faist A 1975 *Nuovo Cimento* B **25** 521–37
Narozhny N B, Sanchez-Mondragon J J and Eberly J H 1980 *Phys. Rev.* A **23** 236–46
Stenholm S 1973 *Phys. Rep.* **6** No 1